Distilling Noise Sources for Digital Capture Devices

Peter D. Burns and Don Williams
Eastman Kodak Company
Rochester, New York

Abstract

A procedure that enables the evaluation and further distillation of fixed pattern noise for digital capture devices is proposed. This method also allows for the direct calculation of the random, or temporal, noise contribution, devoid of fixed pattern components. Our method is consistent with a draft digital camera noise measurement standard under consideration through ISO 15739, but is intended to be a more general approach to the problem. Using common measurement protocols for statistical estimation, a demonstration of the technique for a desktop reflection scanner is provided, accompanied by data analysis. This analysis showed that over 90% of the variance was due to fixed pattern noise. Surprisingly, over 75% was due to the target's microstructure and not the scanner itself. Applications for this method include device performance verification, engineering system analysis, and target noise specification.

Introduction

The analysis of image noise in digital image acquisition systems often focuses on random noise sources,[1-3] such as those associated with quantum signal detection (shot noise) and signal-independent fluctuations (dark current, readout noise, etc.). These sources are often modeled as stochastic sources where the fluctuations introduced are temporally uncorrelated (from image to image). Other important sources of image noise are the pixel-to-pixel sensitivity variations and dark signal sources that introduce repeatable patterns into image data. This *fixed-pattern noise* (FPN) is usually corrected by signal processing based on, e.g., calibration scans of a reference element in a print or film scanner.[4] For digital scanners, which use one-dimensional imaging arrays, this can result in spatially correlated streaks.[5]

There are several reasons why residual fixed-pattern noise is still evident in many stored digital images. Accurate fixed-pattern noise correction requires an assumption or knowledge of the *form* of the source. If the noise is modeled as a variation in photometric response (gain), as is often the case, then the captured image is corrected by multiplying each stored pixel value by the inverse of that gain. If q is the input exposure and g is the imager response gain, then the detected signal at pixel i is[*]

$$x_i = g_i q = (\mu_g + \Delta g_i) q ,\qquad (1)$$

where μ_g is the average or nominal gain, and $q \Delta g_i$ is the fixed pattern error added to the ith pixel. The corrected signal, y, is given by

$$y_i = x_i \frac{\mu_g}{(\mu_g + \Delta g_i)} \qquad (2)$$

Substitution of Eq. (2) into Eq. (1) results in elimination of the fixed-pattern noise

$$y_i = \mu_g q .$$

Note that the correction applied in Eq. (2) is dependent on estimation of Δg_i. If this quantity varies over time, with temperature, or for any other reason, then the correction will be incomplete, resulting in a residual fixed-pattern error. Residual FPN can also be the result of the necessary finite precision used for both storage of the array and computation of Eq. (2). Careful encoding of correction factors can reduce these sources of residual error but not eliminate them.

In field practice, additional noise contributions because of the target (scratches, grain), platen (scratches, dirt), and image processing may also be embedded in the captured image and resulting noise calculation. This is especially a problem for the evaluation of high-resolution film and document scanners where the in-focus microstructure of the film or reflection target inflates the pixel-to-pixel noise statistics. While optical defocus is often offered as a solution, this is frequently unreliable, impractical, or unattainable in non-laboratory environments.

Our approach to the analysis of the various noise sources involves the statistical estimation of the components of what has been called a 'Three-Dimensional Noise Model'.[6] We will limit our attention to the first- and second-order image noise statistics in terms of mean and variance of the pixel values. Interpretation of image noise levels in terms of image quality and comparison of differing scanning parameters generally requires an absolute measure of image noise that includes the spatial extent of the image

---

[*] Here the input exposure, q, is taken as fixed, rather than a random variable subject to shot-noise fluctuations.

sampling, e.g., in terms of variance/mm^2 or noise power spectrum.[2, 7, 8] These topics, however, will not be addressed here.

Theory

For purposes of this paper, a simple additive noise model, which separates effective random and fixed pattern noise (FPN) contributions, is adopted. The pixel variance is taken as the sum of its components,

$$\sigma^2_{total} = \sigma^2_{random} + \sigma^2_{fp} . \qquad (3)$$

Here we do not require all noise sources to be independent and additive; we are merely interested in the effective components as in Eq. (3). Our procedure, therefore, can be seen as the application of variance component analysis[9] to digital image capture[*]. In general, these noise components will vary with (mean) signal or color. In Eq. (3) σ^2_{total} is the mean squared fluctuations observed by calculation of the sample variance over pixels in a nominally uniform area, and σ^2_{random} is the random temporal variance observed from frame-to-frame. The fixed pattern component can be the result of several sources. For a print scanner these can include platen (glass), input target, and imager-induced fluctuations,

$$\sigma^2_{fp} = \sigma^2_{target} + \sigma^2_{platen} + \sigma^2_{imager} . \qquad (4)$$

The analysis and procedure that follow are based on the capturing and processing data, which allow the suppression of one or more of these sources, so that the remaining sources can be estimated. While the second-order statistics of the image noise (variance, rms) are of primary interest, the proposed methods can be generalized to include the autocovariance or noise-power spectrum. The descriptions that follow are for a single image record, which can be repeated for each color-record of interest. Our noise analysis procedure is consistent with a draft digital camera standard[10] (ISO 15739), but is intended to be a more general approach to the problem

Notation

For this report, the following notation is observed whenever possible,

{**x: V**} is a set of replicate image arrays, gathered while varying parameter **V**. For example,

{**x: **} is a set acquired by simple repeated scanning varying only in time,

{**x: target**} a set acquired by moving the target location between each sample image acquisition.

When expressed as a data array, a data set is denoted x_{pqr}, p = 1, …, P pixels, q = 1, …, Q lines, r = 1, …, R replicates. Figure 1 shows the sampling used.

---

[*] Specifically, analysis based on a random effects one-way analysis-of-variance model.
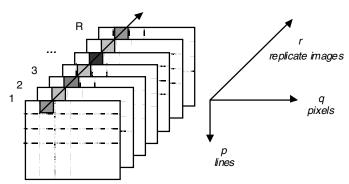

Figure 1. Sets of image data used to estimate fixed pattern and random noise components.

Experimental

Before giving a concise procedure for noise cracking in Section 4, we describe the results of analysis performed for a desktop reflection scanner.

Scanner and Target

A desktop print scanner was selected for testing the noise cracking technique. This is an inexpensive 600 dpi (native) reflection scanner with a trilinear detector array. To minimize data interpretation and complexity for this initial experiment all data was collected in an 8-bit linear (gamma = 1.0) mode for the green channel alone at 600 dpi sampling frequency. No sharpening or auto-balance features were applied. The six Munsell gray patches on a standard Macbeth color checker were used as neutral gray scale target inputs for the testing. These matte samples are considered uniform and are often used for device image noise evaluation.

Data Collection Replicate Scans, {x: } - Total Noise, Random Noise, Fixed Pattern Noise

Before collecting image data, the platen was cleaned, and the scanner was permitted to warm-up for at least one-hour. The target features were then located near the top center of the scanner platen. A set {**x: **} of eight replicate 2-D image records, (R = 8), of the target (neutral photographic step tablet) were then collected under the scanner software conditions stated above. The target was not moved between scans. The image data Region of Interest (ROI) relative to the scanner platen was not changed. Within the return-to-position error of the scanner, each of these scans would ideally be spatially registered. Using the model of Eq. (3), these scans were used to directly calculate the total noise (σ^2_{total}), random noise (σ^2_{random}), and fixed pattern noise, (σ^2_{fp}). In the draft version of ISO 15739 these scans are referred to as temporal scans because they are used to measure the temporal noise. For purposes of this document, the temporal noise is equivalent to random noise.

The set {**x: **} was examined to ensure that replicate scan records exhibited little or no return-to-position errors. Two of the eight image records were deemed misregistered

relative to the others, and discarded. While this task was performed visually with the aid of magnified images in Photoshop software, it could easily be automated with misregistration calculation tools and the correct target features. Six image records were used for the replication scan series ($R = 6$).

Translation Scans, {y: target} – Target and Imager Fixed Pattern Noise

A set **{y: target}** of eight more image records ($R = 8$) were also scanned. Between each of these records, the target was translated slightly in either the fast or slow (horizontal or vertical image-) scan direction. Rotation of the target was avoided. Again, the ROI relative to the scanner platen was not changed. By virtue of this unchanged ROI, each scan was collected using the same portion of the scanning array and platen area, despite seeing a different portion of the target each time. This set of scans was used to separate the target-induced fixed pattern noise from other FPN sources intrinsic to the imager (platen, detector, and illumination).

Two sets of data were extracted from this translation series to arrive at estimates of the target noise and imager FPN. The data set for distilling the target noise was extracted from **{y: target}** by selecting the same ROIs in the gray patches for each image record. Each of these ROIs were captured over the same platen area, with the same region of the scanning array, and over the same greater patch area, albeit with shifted target features. Therefore, the inter-record average of these ROIs for a particular gray patch reduced the random noise and FPN because of the target. This leaves the FPN due to the imager.

The data set for distilling the imager fixed pattern noise *directly* was extracted by selecting an image area for each member of **y** corresponding to the same target patch area. This we denote as **{z: detector}** since, for this set, only the relative position along the detector array was being varied ($R = 8$).

Statistic Calculations and Results

The above gathered data sets were used as diagnostic image files. They were gathered in such a way to aid in the isolation of particular noise component variances. For example, if the influence of target (medium, scratches) noise is to be eliminated from a metric, one could collect a set by moving the target between the capture of each image. This would allow an 'averaging out' of target noise. This process can be seen as part of the estimation procedure for the removal of this component. The complete estimation procedure includes data collection (image sets) and computation of the statistics.

Total Noise Analysis - Total Noise, Random Noise, Fixed Pattern Noise

Consider the task of isolating the random (frame-to-frame temporal) image noise variance from the total variance. As a first step, the total variance was computed over all pixels for each image, for the entire data set of R images. This yields s^2_{total}. After calculating the grand mean

in Eq. (5), the total variance is calculated, in turn, from Eq. (6).

$$\bar{x} = \frac{1}{PQR} \sum_{p=1}^{P} \sum_{q=1}^{Q} \sum_{r=1}^{R} x_{pqr} \tag{5}$$

$$s^2_{total} = \frac{1}{PQR-1} \sum_{p=1}^{P} \sum_{q=1}^{Q} \sum_{r=1}^{R} \left(x_{pqr} - \bar{x} \right)^2 . \tag{6}$$

Equation (6) implies that all pixel data represent independent observations of the underlying random processes (fixed-pattern and random). This is not strictly true, since the effective fixed pattern component is 'observed' R times for a given data set. Inter-record averaging of the R registered records, x_{pqr}, is accomplished accordingly by

$$\bar{x}_{pq} = \frac{1}{R} \sum_{r=1}^{R} x_{pqr} . \tag{7}$$

This provides an estimate of the fixed pattern noise as an array of values. Independent and direct calculation of the statistics of device noise sources was also desired. To this end, direct calculation of random noise was accomplished with the inter-record sample variance computed for each pixel,

$$s^2_{pq} = \frac{1}{R-1} \sum_{r=1}^{R} \left(x_{pqr} - \bar{x}_{pq} \right)^2 . \tag{8}$$

These data were used in a pooled estimate of the random noise variance,

$$s^2_{random} = \frac{1}{PQ} \sum_{p=1}^{P} \sum_{q=1}^{Q} s^2_{pq} . \tag{9}$$

The FPN variance is computed from the array computed in Eqs. (7), and (9)

$$s^2_{fp} = \frac{1}{PQ-1} \sum_{p=1}^{P} \sum_{q=1}^{Q} \left(\bar{x}_{pq} - \left(\frac{1}{PQ} \sum_{p=1}^{P} \sum_{q=1}^{Q} \bar{x}_{pq} \right) \right)^2 - \frac{s^2_{random}}{R} , \tag{10}$$

where the last term of the RHS of Eq. (10) ensures that an unbiased estimate is computed. The two estimated noise variances were then combined to see to what extent Eq. (3) holds for the system under study,

$$s^2_{total} \overset{?}{=} s^2_{random} + s^2_{fp} .$$

The results of the total noise analysis are given in Table 1 and Figure 1. These results show that the sum of estimated random and total FPN variances closely matches the independently measured total noise estimate, as predicted by the model of Eq. 3. The morphology and magnitude of these plots also offer insight into the scanning process. Note that nearly all of the total noise is accounted for by the FPN estimate. In addition, an oddly behaved point occurs at a

mean count value of 25 on the total FPN curve that, in turn, cascades into the total noise estimate. Insight into these behaviors can be analyzed by further distilling the total FPN contribution. This is possible by interrogating the **{y: target}** data set. This analysis follows.
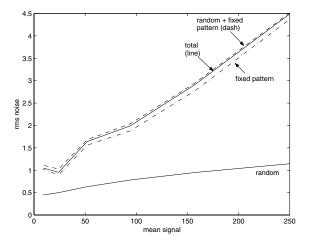

Figure 2. Component noise analysis for desktop scanner

Total FPN Analysis- Target FPN, Imager FPN

Recall that each of the ROIs for **{y: target}** were captured over the same platen area and with the same region of the scanning array, but with shifted target features. Therefore, the inter-record average of these ROIs for a particular gray sample will reduce both random noise and FPN due to the target. This leaves the FPN due to the imager, as expressed in Eqs. (11) and (12)

$$\bar{y}_{pq} = \frac{1}{R}\sum_{r=1}^{R} y_{pqr} \qquad (11)$$

$$s_{imager}^2 = \frac{1}{PQ-1}\sum_{r=1}^{R} (y_{pqr} - \bar{y}_{pq})^2 \qquad (12)$$

Because each image record was spatially shifted on the scanner platen between scans, inter-record averaging over the same physical area of each gray patch reduces both FPN due to the imager, and random noise. The remaining noise is due strictly to the FPN of the target itself. This portion of the analysis extends the recommendations of draft ISO 15739 to further analyze fixed pattern noise.

The breakdown of the fixed pattern noise sources is shown in and Figure 2. Except for the points at mean signal level 250, the agreement between the directly measured total FPN and that calculated from the sum of its measured components is excellent, as expected. In all likelihood, the disagreement of the one point is due to poor ROI registration accuracy for that gray patch with respect to the target FPN data. The averaging calculation of misregistered records will tend to underestimate the real FPN.

Figure 2 also reveals the contribution of the target to the FPN as well as the source of the oddly behaved value at count 25. The magnitude of the target's contribution to the measured FPN is cause for concern in our existing measurement protocols for digital capture devices such as film and document scanners. Over 90% of the total variance was due to FPN. Of this, over 75% was due to the target's microstructure and not the scanner itself.

While target structure contributions can be avoided in laboratory practice, doing so in the field (e.g., competitive assessment, QA testing) is difficult at best and typically unattainable. The low FPN point at count 25 is traceable to the target itself. While the target patch for that point does not appear particularly noise free, its source may likely be from simple manufacturing variability. Whatever the source, the noise cracking technique applied here was able to detect it.
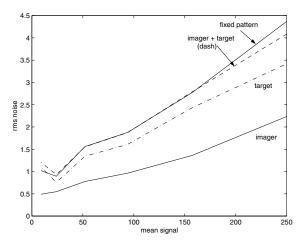

Figure 3. Target and imager components of fixed pattern noise

Finally, some ambiguity remained on the further distillation of the combined imager (platen+CCD) FPN. While not able to directly measure both of these contributors, the hypothesis that the "combined" noise was due to the linear imager itself was tested. Using the image data from the directly measured imager FPN, pixel averaging in the slow scan direction of the CCD was done. This created an image vector that characterized the FPN of the linear CCD alone. Calculating the noise along this vector for each gray patch revealed identical data to that of the measured imager FPN for a 2-D field. By deduction then, neither the platen itself, nor slow-scan effects of the CCD contributed anything to the total FPN. All imager FPN variance was due to the pixel-pixel fluctuations along the linear CCD array.

Conclusions

A data capture and processing method for separating the components of fixed pattern noise in digital capture devices has been proposed and demonstrated. The method can be based on a single set of replicate images **{x: }** for separation of random and fixed-pattern noise statistics. If a second set

is added, **{y: target}**, the fixed pattern noise can be further separated into components due to imager and target.

The method was tested on a common 600 dpi flatbed reflection scanner with standard field capture protocols. Using well-accepted additive noise models, very good agreement between explicit noise calculations and algebraically inferred ones was reached. This revealed that existing field practices for measuring noise of document and film scanners might need to be reconsidered in light of the fixed pattern noise caused by the target alone. For the device tested, nearly 75 percent of the total noise was due to target FPN.

This method can be used for scanner and digital camera performance verification, fixed-pattern correction evaluation, and target noise specification. The above can be done as part of engineering evaluation and to track changes to device characteristics (deterioration) in the field. Because an intermediate result is an array representing fixed pattern noise as a function of image location, the method could also form part of a method to update fixed-pattern gain data.

Acknowledgement

We would like to thank Eric Sztanko for his contributions to several discussions, while he was developing a Matlab implementation of the noise analysis procedure.

References

1. J. R. Janesick et al., *Opt. Eng.,* **26**, 692-714 (1987).
2. P. D. Burns, Image Signal Modulation and Noise Characteristics of Charge-Coupled Device Imagers, *Proc. SPIE*, **1071**, pg. 144-152, (1989).
3. C. S. McCurnin, L. C. Schooley and G. R. Sims, Charge-Coupled Device Signal Processing Models and Comparisons, *J. Electronic Imaging*, 2, pg. 100-107, (1993).
4. R. Gann, *Desktop Scanners: image quality evaluation*, Prentice Hall PTR, Upper Saddle River, NJ, 1999, pp. 129-13.
5. ibid, ch. 16.
6. G. C. Holst, *Electro-Optical Imaging System Performance*, JCD Publishing, Winter Perk, FL, 1995, pg. 383-387.
7. R. Shaw, Satisfying Simultaneous Resolution and Noise Criteria in Digital Images, *Proc. PICS*, IS&T, pg. 71-74, (2000).
8. P. J. Kane, et al., Quantification of Banding, Streaking and Grain in Flat Fields, *Proc. PICS*, IS&T, pg. 79-83, (2000).
9. R. E. Walpole and R. H. Meyers, *Probability and Statistics for Engineers and Scientists*, 2nd Ed., Macmillan Publishing, New York, 1978, pg. 396-402.
10. ISO/DIS 15739, Photography – Electronic still picture cameras, working draft, ISO/TC42, 4/29/2000, available from Photog. and Imaging Man. Assoc. (PIMA) web site.

Biographies

Peter Burns studied Electrical and Computer Engineering at Clarkson University, receiving his BS and MS degrees. In 1997 he completed his Ph.D. in Imaging Science at Rochester Institute of Technology, where he is a member of the adjunct faculty. After working for Xerox, he joined Eastman Kodak's Imaging Research and Development organization. A frequent contributor to imaging conferences, his technical interests include; system evaluation, simulation, and the statistical analysis of error in digital and hybrid systems. peter.burns@kodak.com

Don Williams received both B.Sc. and M.Sc. degrees in Imaging Science from RIT, and works in Imaging Research and Development at Kodak. His work at Kodak focuses on quantitative signal and noise performance metrics for digital capture imaging devices and imaging system simulations. He has been active for several years in the development of imaging standards, and currently co-leads the PIMA/IT10 effort for both digital print scanner (ISO 16067-1) and digital film scanner (ISO 16067-2) resolution measurement. Mr. Williams is also a frequent contributor and advisor on digitization fidelity issues for the library and museum communities.